International Journal of Electrical, Electronic and Communication Sciences
ISSN: 2517-9438
Vol:12, No:10, 2018

Comparison of the Thermal Characteristics of Induction Motor, Switched Reluctance Motor and Inset Permanent Magnet Motor for Electric Vehicle Application

Sadeep Sasidharan, T. B. Isha

***Abstract*—**Modern day electric vehicles require compact high torque/power density motors for electric propulsion. This necessitates proper thermal management of the electric motors. The main focus of this paper is to compare the steady state thermal analysis of a conventional 20 kW 8/6 Switched Reluctance Motor (SRM) with that of an Induction Motor and Inset Permanent Magnet (IPM) motor of the same rating. The goal is to develop a proper thermal model of the three types of models for Finite Element Thermal Analysis. JMAG software is used for the development and simulation of the thermal models. The results show that the induction motor is subjected to more heating when used for electric vehicle application constantly, compared to the SRM and IPM.

***Keywords*—**SRM, induction motor, IPM, thermal analysis, loss models, electric vehicles.

I. Introduction

ELECTRIC vehicles have gained profound attention in the modern era. This is mainly due to the constraints of pollution that has been caused by the existing internal combustion engines. One of the major drawbacks associated with an electric vehicle is the failure in analyzing the thermal characteristics of the electric motoring unit. This leads to reduced life of the motoring unit and causes unsurety in identifying the stresses associated with the rise in temperature. A proper thermal analysis of the motoring system hence helps in reducing the thermal losses associated with the system thereby increasing the efficiency of the motor. For an electric vehicle, even a little improvement in efficiency can be a handful.

Various motors like induction motors, permanent magnet synchronous motors, SRMs, etc. have been tried and tested for electric traction application. Induction motors are the simplest and age-old motoring unit which is used extensively for traction applications. But, the presence of windings on both the stator and the rotor causes the system to heat heavily during steady state operation which causes increased losses and reduced efficiency of the system at steady state. Also, there is rapid decrease in the life of the motor due to the rise in heat in both the windings. The next candidate extensively used in electric vehicle applications is PMSM. The motor has very high efficiency due to limited losses in the system owing to the absence of rotor windings. The motor uses a permanent magnet as the rotor. But, the properties of the magnet changes due to the rise in temperature of the motor when the system is run at steady state over a longer period. This in turn causes the failure of permanent magnet, and the user has no other option but change the permanent magnet. The motor that has been researched upon but still limited to the electric vehicle application is the SRM. The limitation has been mainly due to the higher amount of torque ripple and acoustic noise associated with the system. Several studies and researches are going on in reducing the torque ripple and noise in the SRM both at the design and control level. But, when the thermal characteristic of the SRM is considered, the motor outdoes the other available motors due to the absence of windings on the rotor. Hence, the rise in temperature in the motor is limited and this in turn gives higher efficiency at steady state for the SRM. Over a long run, SRM gives the highest life compared to the other motors used for electric vehicle application.

The automotive industry is in transition to electric vehicle propulsion. This has made the thermal studies of the electric motors all the more important. In literature, a lot of research has been done in the proper management of the thermal characteristics of the electric motor which is shown to achieve the increased life and power density [1]. This has been the case with various researchers focusing on temperature rise problems associated with electric machines [2]-[4]. Likewise, complex and bulky cooling systems have been introduced in electric vehicles which take up a lot of space in the vehicle [5]-[9]. In the latter half of the 20th century, SRMs were identified as ideal candidates for electric vehicle propulsion owing to its simplicity, robustness, and better thermal characteristics [10]-[12]. Thermal analysis studies have been carried out on SRMs recently [13]-[15]. One such study compared the performance of a 10-hp induction motor with that of a 10-hp SRM [16]. This study showed lower temperature rise in SRMs compared to induction motors. Some of the studies focused on the losses resulting in the switched reluctance owing to temperature rise [17]. More recently, Finite Element analysis of SRMs has eased the thermal analysis of the motor [18].

This work is targeted at the thermal analysis of a SRM and its comparison with a PMSM of similar rating. The analysis is done by Finite element method using the JMAG software. Dominance of the thermal profile of SRM over PMSM is

Sadeep Sasidharan is with the Amrita Vishwa Vidyapeetham, India (e-mail: sadeepsasidharan@gmail.com).

shown using the FEA simulation. Once the comparison has been made, the thermal profile of SRM is analyzed. A cooling system to improve the thermal profile of the SRM is implemented.

This paper is arranged in five sections. Mathematical model of the SRM with losses is given in Section II. Section III gives the model structure for IM, SRM and PMSM. Thermal analysis using JMAG and the performance comparison of the motors is shown in Section IV followed by conclusion and future scope in Section V.

II. Modeling of SRM

SRM is a doubly salient machine and the model of SRM is highly non-linear due to the influence of magnetic saturation. Since the interaction of phase torques is minimal, there is phase torque superposition. A conventional 8/6 SRM is shown in Fig. 1. The principle of operation of a SRM is based on the change in reluctance path when a stator phase is energized at a time.

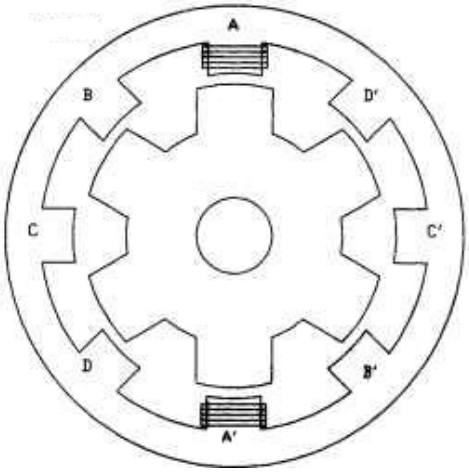

Fig. 1 A conventional 8/6 SRM

The phase equation for a 8/6 SRM is given by

$$V_{a,b,c,d} = r_s i_{a,b,c,d} + \frac{d\lambda_{a,b,c,d}(\theta_r, i_{a,b,c,d})}{dt} \quad (1)$$

where a, b, c and d are the phases of the SRM.

The mechanical motion equation is given by

$$J\frac{d\omega_r}{dt} = T_e - T_l \quad (2)$$

Considering 'a' phase,

$$V_a = r_s i_a + \frac{\partial \lambda_a}{\partial i_a}\frac{di_a}{dt} + \frac{\partial \lambda_a}{\partial \theta_r}\frac{d\theta_r}{dt} \quad (3)$$

$\frac{\partial \lambda_a}{\partial i_a}$ – Transient inductance L_a

$\frac{\partial \lambda_a}{\partial \theta_r}\frac{d\theta_r}{dt}$ – Back emf (E_a)

$\frac{d\theta_r}{dt}$ - ω_r

$$E_a = \frac{\partial \lambda_a}{\partial \theta_r}\omega_r \quad (4)$$

$$V_a = r_s i_a + L_a(\theta_r i_a)\frac{di_a}{dt} + E_a(\omega_r, \theta_r, i_a) \quad (5)$$

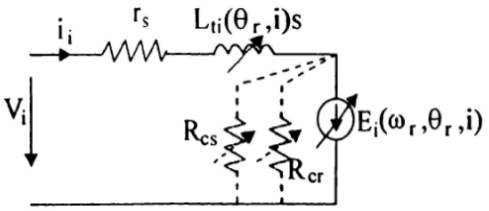

Fig. 2 Equivalent circuit of SRM with core losses

Fig. 2 gives the equivalent circuit of the SRM with loss components. The main losses associated with a SRM are the iron losses associated with the stator and rotor core and the resistive losses associated with the windings in the stator. The losses in a SRM cannot be calculated accurately due to the highly nonlinear nature of the machine. Different types of analysis can be used to obtain the thermal profile of the SRM. Finite element analysis using JMAG is preferred here owing to its higher accuracy in calculations.

Core loss in SRM is given by

$$W_c = K_e f^2 B^2 + K_h f B^{(a+bB)} \quad (6)$$

K_e, K_h, a, b are the constants.

Copper loss in SRM is given by

$$P_{cu} = q I^2{}_{rms} R_s \quad (7)$$

where 'q' is the number of phases in the stator

$$I_{rms} = \frac{I_p}{\sqrt{q}} \quad (8)$$

I_p is the peak current

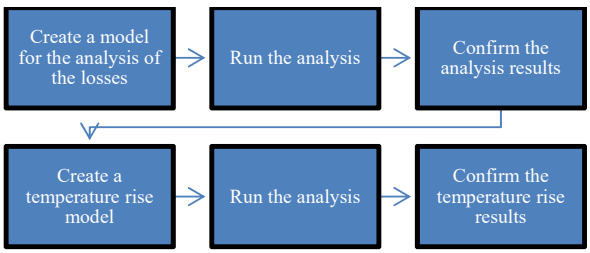

Fig. 3 Thermal analysis flowchart

III. Thermal Analysis of IM, SRM and IPM

A proper model of the motors for comparison has to be developed for performing the thermal analysis. The 20-kW models of the Induction motor, IPM and SRM are shown in Figs. 4 (a), 5 (a), and 6 (a). The mesh models developed for

the finite thermal analysis of the model are shown in Figs. 4 (b), 5 (b) and 6 (b), respectively.

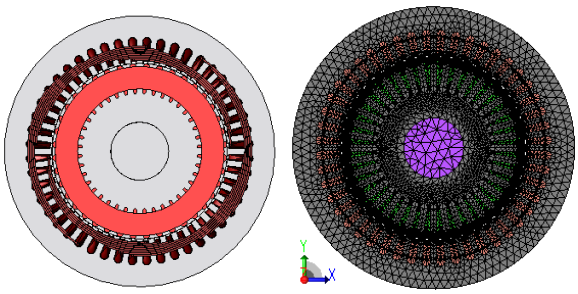

(a) (b)

Fig. 4 Induction motor; (a) Normal structure (b) Mesh structure for thermal analysis

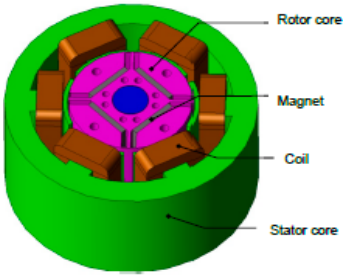

(a)

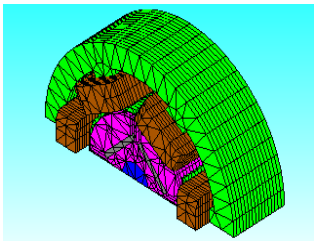

(b)

Fig. 5 SRM; (a) Normal structure (b) Mesh structure for thermal analysis

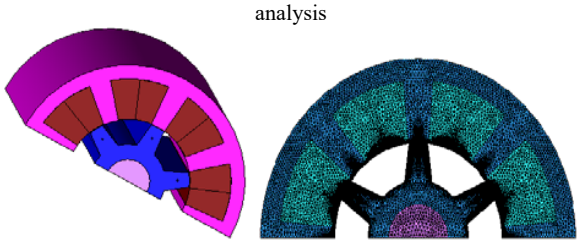

(a) (b)

Fig. 6 IPM; (a) Normal Structure (b) Mesh structure for thermal analysis

IV. Results and Discussion

A. Induction Motor

The temperature analysis model gives the thermal curve of the induction motor as shown in Fig. 7. The curve shows maximum heating of the motor in the rotor windings when the temperature model system is run for 7000 s. The rotor core is also heated to a very high value. Constant usage of induction motor creates a possibility of excessive heat in the rotor and development of the thermal spots leads to the failure of the induction motor. The stator core is found to heat but with a lesser temperature effect.

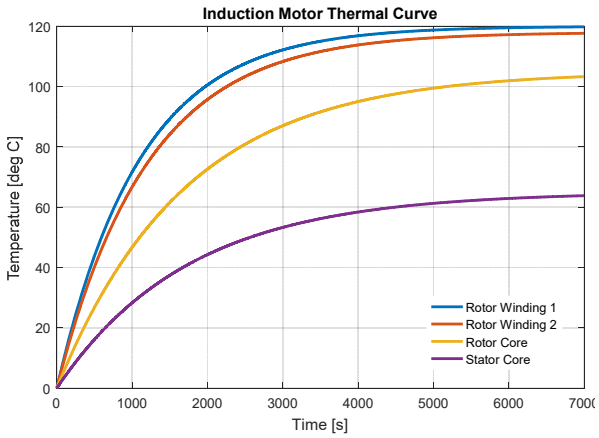

Fig. 7 Thermal analysis curve for IM

B. IPM

The thermal curve of the IPM model is obtained after running the temperature model for 7200 s. The temperature model is arrived at from the loss model. The copper and iron loss models are shown in Figs. 8 and 9. The IPM motor has less loss pertaining to the absence of windings in the system. The coil present in the stator is the part that gets heated fasted and the maximum temperature is found to be 42 °C as seen in Fig. 10. The rest of the major components like the stator, rotor and the magnet are least affected by constant running of the IPM. But, there is a higher probability of the magnetic properties to be altered in case of constant running of the IPM. This can cause the motor characteristics to behave in a different way from the normal.

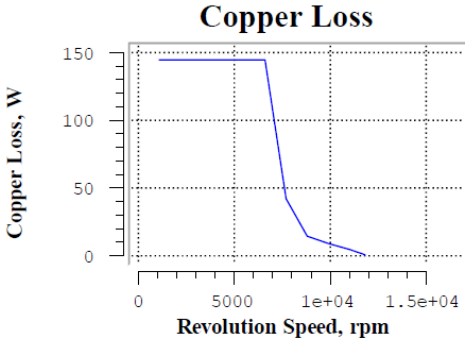

Fig. 8 Copper loss for the IPM

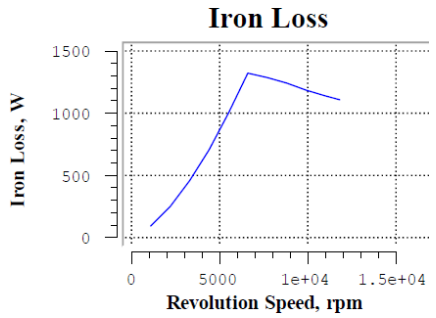

Fig. 9 Iron loss for the IPM

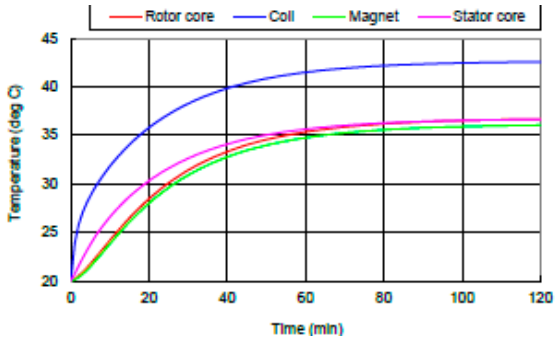

Fig. 10 Thermal analysis curve for IPM

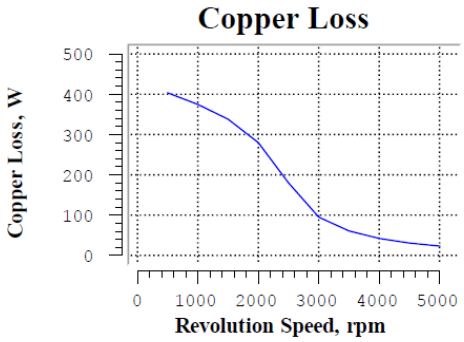

Fig. 11 Copper loss in SRM

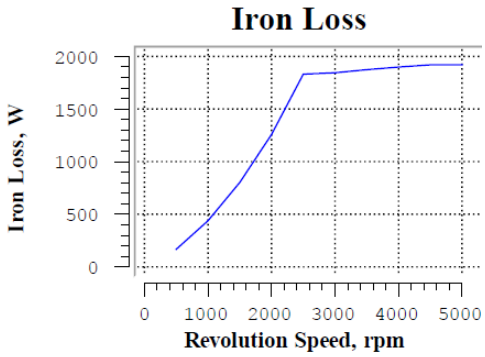

Fig. 12 Iron loss in SRM

C. SRM

The SRM temperature model is realized from the loss model of the SRM. The copper loss is very low because of the absence of windings in the rotor as shown in Fig. 11. The major loss is the iron loss as shown in Fig. 12. The thermal analysis curve in Fig. 13 shows the maximum heating happening in the stator where the coils are present. When SRM is considered, another factor called the switching of the motor has to be considered. The switching loss is high, and this can lead to the reduced life of the switches as shown in Fig. 13. But, the switches do not have an impact on the thermal nature of the SRM.

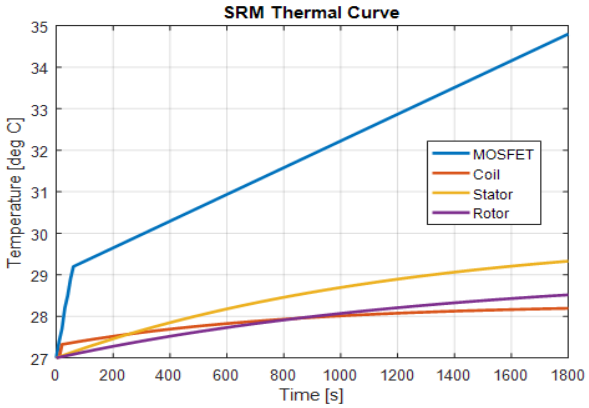

Fig. 13 Thermal curve with respect to temperature

Table I gives the specifications of the Induction motor, SRM and IPM motor used for the thermal study. The power rating is set as 20 kW for the comparison. The speed reference is also the same at 1500 rpm. The motors are having the same outer diameter for comparison.

TABLE I
MOTOR SPECIFICATIONS

Machine Specifications	Induction Motor	SRM	IPM Motor
Power	20kW	20kW	20kW
Speed	1500rpm	1500rpm	1500rpm
Voltage	400V	400V	400V
Torque	120Nm	150Nm	40.3Nm
Efficiency	81.23	88.74	95.1
Stack length	250mm	250mm	250mm
Air gap	0.23	0.23	0.23
Outer diameter	250mm	250mm	250mm

The losses occurring in each of the motors for a small running duration are shown in Table II. It can be seen that the temperature does not affect the system much in this scenario. Here, the induction motor is seen to give the highest loss and the IPM motor is seen to give the least. The higher loss in the induction motor is due to the presence of windings in the stator which leads to a higher copper loss. The IPM motor is seen to have the lowest iron loss, whereas the SRM is found to have the highest iron loss for a smaller duration of operation. Because of the higher losses, the induction motor is seen to have the lowest efficiency among the three motors.

The losses with temperature effect for the three motors are shown in Table III. The machine is run for a time duration of 7000 s for this analysis. It is seen that the induction motor has

the maximum heating effect when compared with the other two motors. This is due to the presence of the windings on the stator and rotor which accounts for a higher loss when the stator and rotor resistance are changed with respect to the temperature at each iteration in the simulation. The permanent magnet motor is having the lowest losses owing to the lack of any major windings in the motor. The SRM is seen to have a higher iron loss and lesser copper loss due to the absence of rotor windings. The IPM has the highest efficiency with the temperature effect because of the reduced loss in the motor.

TABLE II
LOSSES WITHOUT TEMPERATURE EFFECT

	Induction Motor (Watts)	SRM (Watts)	IPM Motor (Watts)
Iron loss	1659	2200	144
Copper loss	1357	400	150
Total loss	3016	2600	294
Efficiency	81.23	88.74	95.1

TABLE III
LOSSES WITH TEMPERATURE EFFECT

	Induction Motor (W)	SRM (W)	IPM Motor (W)
Iron loss	2254	2651	1457
Copper loss	1987	798	569
Total loss	4241	3449	2026
Efficiency	73.9	81.2	88.7

V. CONCLUSIONS AND FUTURE SCOPE

A 20 kW, 8/6 SRM, IM and IPM were modeled using JMAG Designer. The major geometrical dimensions were calculated based on the theoretical design. A mathematical model of the SRM was developed for thermal analysis. The IPM and IM thermal models were considered based on their existing models. The machines were simulated using the JMAG Finite Element Thermal Analysis. The results showed the dominance of the SRM and IPM when compared to IM in their excellent thermal characteristics. A laboratory model of the prototype SRM, IM and IPM is under consideration for experimental validation. Performance analysis due to the deterioration of the magnetic nature of the IPM also can be considered as a future scope.

REFERENCES

[1] Bilgin, B. and Emadi, A., 2014. Electric motors in electrified transportation: A step toward achieving a sustainable and highly efficient transportation system. *IEEE Power Electronics Magazine*, *1*(2), pp.10-17

[2] Compton, F. A., 1943. Temperature limits and measurements for rating of DC machines. *Electrical Engineering*, *62*(12), pp.780-785.

[3] Hughes, E., 1924. The rise and distribution of temperature in small electrical machines. *Journal of the Institution of Electrical Engineers*, *62*(331), pp.628-648.

[4] Kennelly, A. E., 1926. Can the thermal capacity of electric machines: Be made a simple and practical element of rating?. *Journal of the AIEE*, *45*(5), pp.438-445.

[5] Kral, C., Haumer, A. and Bauml, T., 2008. Thermal model and behavior of a totally-enclosed-water-cooled squirrel-cage induction machine for traction applications. *IEEE Transactions on Industrial Electronics*, *55*(10), pp.3555-3565.

[6] Li, Z., Fu, D., Guo, J., Gu, G. and Xiong, B., 2009, November. Study on spraying evaporative cooling technology for the large electrical machine. In *Electrical Machines and Systems, 2009. ICEMS 2009. International Conference on* (pp. 1-4). IEEE.

[7] Marignetti, F., 2010. On liquid-nitrogen-cooled copper-wound machines with soft magnetic composite core. *IEEE Transactions on Industry Applications*, *46*(3), pp.984-992.

[8] Richards, P. B., 1958. Progress in the thermal design of oil-cooled rotating electric machines. *Transactions of the American Institute of Electrical Engineers, Part II: Applications and Industry*, *77*(5), pp.330-334.

[9] Zheng, P., Liu, R., Thelin, P., Nordlund, E. and Sadarangani, C., 2008. Research on the cooling system of a 4QT prototype machine used for HEV. *IEEE transactions on energy conversion*, *23*(1), pp.61-67.

[10] Balamurugan, S. and Sumathi, P., 2004, November. Analysis of temperature rise in switched reluctance motor due to the core and copper loss by coupled field finite element analysis. In *Power System Technology, 2004. PowerCon 2004. 2004 International Conference on* (Vol. 1, pp. 630-634). IEEE.

[11] Lovatt, H. C., McClelland, M. L. and Stephenson, J. M., 1997. Comparative performance of singly salient reluctance, switched reluctance, and induction motors.

[12] Rahman, K. M., Fahimi, B., Suresh, G., Rajarathnam, A. V. and Ehsani, M., 2000. Advantages of switched reluctance motor applications to EV and HEV: Design and control issues. *IEEE transactions on industry applications*, *36*(1), pp.111-121.

[13] Harris, M. R. and Miller, T. E., 1989, September. Comparison of design and performance parameters in switched reluctance and induction motors. In *Electrical Machines and Drives, 1989. Fourth International Conference on* (pp. 303-307). IET.

[14] Inamura, S., Sakai, T. and Sawa, K., 2003. A temperature rise analysis of switched reluctance motor due to the core and copper loss by FEM. *IEEE Transactions on Magnetics*, *39*(3), pp.1554-1557.

[15] Moghbelli, H., Adams, G. E. and Hoft, R. G., 1991. Performance of a 10-Hp switched reluctance motor and comparison with induction motors. *IEEE Transactions on Industry Applications*, *27*(3), pp.531-538.

[16] Sadeep Sasidharan, Isha T. B, "SRM for EV: The Future", *PESTSE*, 2018

[17] Rouhani, H., Faiz, J. and Lucas, C., 2007. Lumped thermal model for switched reluctance motor applied to mechanical design optimization. *Mathematical and computer modelling*, *45*(5-6), pp.625-638.

[18] Wu, W., Dunlop, J. B., Collocott, S.J. and Kalan, B. A., 2003. Design optimization of a switched reluctance motor by electromagnetic and thermal finite-element analysis. *IEEE Transactions on Magnetics*, *39*(5), pp.3334-3336.